



Structurally Diverse Polyketides From the Mangrove-Derived Fungus *Diaporthe* sp. SCSIO 41011 With Their Anti-influenza A Virus Activities

Xiaowei Luo^{1,2†}, Jie Yang^{3†}, Feimin Chen³, Xiuping Lin¹, Chunmei Chen^{1,2}, Xuefeng Zhou^{1,2*}, Shuwen Liu^{3,4*} and Yonghong Liu^{1,2*}

¹ CAS Key Laboratory of Tropical Marine Bio-Resources and Ecology, Guangdong Key Laboratory of Marine Materia Medica, South China Sea Institute of Oceanology, Chinese Academy of Sciences, Guangzhou, China, ² University of Chinese Academy of Sciences, Beijing, China, ³ Guangdong Provincial Key Laboratory of New Drug Screening, Guangzhou Key Laboratory of Drug Research for Emerging Virus Prevention and Treatment, School of Pharmaceutical Sciences, Southern Medical University, Guangzhou, China, ⁴ State Key Laboratory of Organ Failure Research, Southern Medical University, Guangzhou, China

OPEN ACCESS

Edited by:

Xian-Wen Yang,
Third Institute of Oceanography, State
Oceanic Administration, China

Reviewed by:

Christophe Salome,
SpiroChem AG, Switzerland
Rongbiao Pi,
Sun Yat-sen University, China

*Correspondence:

Xuefeng Zhou
xfzhou@scsio.ac.cn
Shuwen Liu
liusw@smu.edu.cn
Yonghong Liu
yonghongliu@scsio.ac.cn

[†]These authors have contributed
equally to this work.

Specialty section:

This article was submitted to
Medicinal and Pharmaceutical
Chemistry,
a section of the journal
Frontiers in Chemistry

Received: 07 May 2018

Accepted: 22 June 2018

Published: 12 July 2018

Citation:

Luo X, Yang J, Chen F, Lin X, Chen C,
Zhou X, Liu S and Liu Y (2018)
Structurally Diverse Polyketides From
the Mangrove-Derived Fungus
Diaporthe sp. SCSIO 41011 With
Their Anti-influenza A Virus Activities.
Front. Chem. 6:282.
doi: 10.3389/fchem.2018.00282

Influenza A virus (IAV) is a severe worldwide threat to public health and economic development due to its high morbidity and mortality. Marine-derived fungi have been evidenced as a prolific source for the discovery of pharmacologically-active lead compounds. During the course of our search for novel bioactive substances from marine microorganisms, six new polyketides, including two octaketides (**1–2**), one chromone derivative (**13**), two highly substituted phthalides (**17–18**), and one α -pyrone derivative (**21**) along with 22 known congeners were isolated from a mangrove-associated fungus *Diaporthe* sp. SCSIO 41011. Their structures were determined by spectroscopic analysis and by comparison with literature data. And the absolute configurations were established according to the specific rotation or electron circular dichroism method. Antiviral evaluation results revealed that compounds **14**, **15**, **26**, and 5-chloroisorotiorin displayed significant anti-IAV activities against three influenza A virus subtypes, including A/Puerto Rico/8/34 H274Y (H1N1), A/FM-1/1/47 (H1N1), and A/Aichi/2/68 (H3N2), with IC₅₀ values in the range of 2.52–39.97 μ M. The preliminary structure-activity relationships (SARs) are also discussed. These findings expand the chemical and bioactive diversity of polyketides derived from the genus *Diaporthe*, and also provide a basis for further development and utilization of chromone, xanthone, and chloroazaphilone derivatives as source of potential anti-viral chemotherapy agents.

Keywords: *Diaporthe* sp., polyketides, cytosporones, phthalides, anti-influenza A virus

INTRODUCTION

Polyketides represent an important category of secondary metabolites with great structural diversity from simple aromatics to highly modified complex architectures, such as macrolides, polyphenols, polyethers, polyenes, and enediynes (Fujii, 2010; Zheng et al., 2015). Distributing broadly in microbial origins, they are constructed by combination of iterative polyketide synthases (PKSs) and multifunctional and iterative oxygenases (Hang et al., 2016). In addition,

polyketides play a vital role in modern medicine due to their diverse pharmacological features, such as lovastatin, a well-known fungal polyketide statin functioned as a cholesterol-lowering agent (Crawford and Townsend, 2010). Belonging to the family of octaketides, biosynthetically related cytosporones, dothiorelones and phomopsins are characterized with a di-/tri-hydroxybenzene lactone or a resorcinol scaffold harboring an *n*-heptane substituent, which were mainly encountered in endophytic fungi of several genera, such as *Phomopsis* (Kornsakulkarn et al., 2015; Kongprapan et al., 2017; Tan et al., 2017), *Diaporthe* (Brady et al., 2000; Liu et al., 2018), *Cytospora* (Brady et al., 2000; Abreu et al., 2010), *Pestalotiopsis* (Xu et al., 2009b). Of special note, cytosporone B (7) was reported as a nuclear orphan receptor Nur77 agonist as a promising therapeutic drug for cancers and hypoglycemia (Zhan et al., 2008), as well as the transcription factor NR4A1 agonist to control IAV infection and improve pulmonary function in infected mice (Xia et al., 2013; Egarnes et al., 2017), which had aroused a great interest for chemical synthesis study (Von Delius et al., 2017).

Influenza A virus (IAV), a negative sense RNA virus, is one of the main causes of human acute respiratory diseases characterized with high morbidity and mortality, posing a serious threat to public health and economic development (Liu et al., 2017). IAVs repeatedly circulate in many animal hosts, such as humans, birds, horses, dogs, and pigs, which can be subtyped to two envelope proteins: haemagglutinin (HA) and neuraminidase (NA) glycoproteins according to the antigenic properties (Medina and Garcia-Sastre, 2011). In 2009, the pandemic influenza H1N1 virus rapidly spread to 214 countries around the world, causing human infection and acute respiratory illness of more than 17,700 deaths (Bautista et al., 2010). As of 25th April 2018, there have been reported 1625 confirmed cases of human H7N9 infection and 623 deaths since 2013 according to the World Health Organization (http://www.fao.org/ag/againfo/programmes/en/empres/H7N9/situation_update.html). However, two families of antiviral drugs are hitherto currently used to treat human IAV infections, which are NA inhibitors, like zanamivir and oseltamivir, and inhibitors of the viral M2 protein exemplified by amantadine and rimantadine (Medina and Garcia-Sastre, 2011; Song et al., 2015). Due to the emergence of drug-resistant viral strains, there is an urgent development for novel classes of anti-IAV agents with new mode of action.

Marine-derived fungi are reported as a prodigious source of development for new antivirals against different important viruses (Moghadamtousi et al., 2015). In our continuing endeavor to discover biologically active compounds from marine microbes, a series of structurally interesting and biologically active natural products have been described (Luo et al., 2017; Tan et al., 2018). Recently, six new cytotoxic chloroazaphilone derivatives, isochromophilones A–F, have been isolated from the fungus *Diaporthe* sp. SCSIO 41011, an endophytic fungus obtained from the fresh tissue of the marine mangrove plant *Rhizophora stylosa* (Luo et al., 2018). Subsequent chemical investigations on the remaining fractions of the fungus led to the isolation of structurally diverse aromatic polyketides, including

octaketides (dothiorelones or cytosporones), phthalides, chromones, xanthenes, etc. (Figure 1). The structures of these compounds were determined by physicochemical properties and spectral data analysis as well as comparison with those reported in the literature. All the compounds were examined for anti-IAV activities against three influenza A virus subtypes, including A/Puerto Rico/8/34 H274Y (H1N1), A/FM-1/1/47 (H1N1), and A/Aichi/2/68 (H3N2). Details of the isolation, structure elucidation, and biological activity of these compounds, as well as preliminary SARs, are reported herein.

MATERIALS AND METHODS

General Experimental Procedures

Semi-preparative HPLC was performed on a Hitachi Primaide apparatus using an ODS (octadecylsilanized silica) column (YMC-pack ODS-A, YMC Co. Ltd., 10 × 250 mm, 5 μm, 2.5 mL/min). Chiral HPLC separation was performed using CHIRALPAK IC column (250 × 4.6 mm, 5 μm). TLC and column chromatography (CC) were performed on plates precoated with silica gel GF254 (10–40 μm) and over silica gel (200–300 mesh) (Qingdao Marine Chemical Factory), and Sephadex LH-20 (Amersham Biosciences), respectively. Spots were detected on TLC (Qingdao Marine Chemical Factory) under 254 nm UV light. All solvents employed were of analytical grade (Tianjin Fuyu Chemical and Industry Factory). The NMR spectra were obtained on a Bruker Avance spectrometer (Bruker) operating at 500 and 700 MHz for ¹H NMR, 125 MHz, and 175 MHz for ¹³C NMR, using TMS as an internal standard. Optical rotations were acquired using a Perkin Elmer MPC 500 (Waltham) polarimeter. HRESIMS and ESIMS spectra data were recorded on a MaXis quadrupole-time-of-flight mass spectrometer and an amaZon SL ion trap mass spectrometer (Bruker), respectively. UV spectra were recorded on a Shimadzu UV-2600 PC spectrometer (Shimadzu). ECD spectra were performed on a Chirascan circular dichroism spectrometer (Applied Photophysics). IR spectra were measured on an IR Affinity-1 spectrometer (Shimadzu). The artificial sea salt was a commercial product (Guangzhou Haili Aquarium Technology Company).

Fungal Material

The fungus *Diaporthe* sp. SCSIO 41011 had the same origination as that in our recent published paper (Luo et al., 2018). A voucher specimen was deposited in the CAS Key Laboratory of Tropical Marine Bio-resources and Ecology, South China Sea Institute of Oceanology, Chinese Academy of Sciences, Guangzhou, China.

Extraction and Isolation

The fermentation of the strain and the extraction and isolation of its extract was identical to that of our recent published paper (Luo et al., 2018). Briefly, nine fractions was isolated from the EtOAc extract (150 g) by silica gel vacuum liquid chromatography (VLC) using step gradient elution with petroleum ether/CH₂Cl₂ (0–100%). Compounds **23** (40 mg, *t*_R 30 min) and **25** (4.5 mg, *t*_R 18 min) were purified from Fr.2 (13 g) by an ODS column (MeOH/H₂O: 10–100%) and followed by semiprep-HPLC with

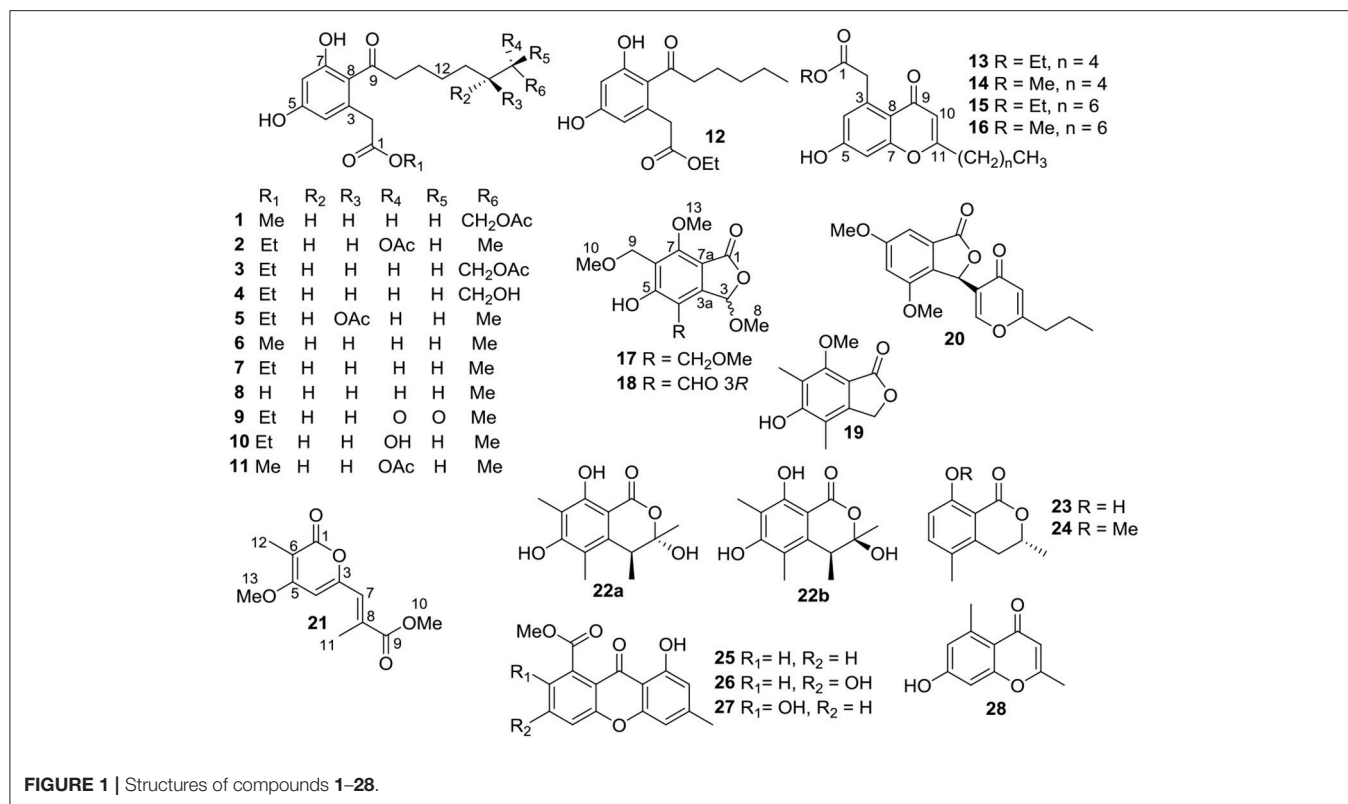


FIGURE 1 | Structures of compounds 1–28.

72% (2.5 mL/min) and 50% MeCN (2.3 mL/min) elutions, respectively. Fr.3 (10 g) was purified on Sephadex LH-20 (MeOH), an ODS column (MeOH/H₂O: 10–100%) and finally semiprep-HPLC (70% MeCN, 2.3 mL/min) to afford compounds **17** (4.2 mg, *t_R* 7 min) and **24** (3.5 mg, *t_R* 9 min). Fraction 4 (12 g) was subjected to Sephadex LH-20 (MeOH) to provide eight subfractions (Frs.4-1~4-8). Then ten subfractions (Frs.4-3-1~4-3-10) were obtained from Fr. 4-3 by an ODS column (MeOH/H₂O: 10–100%). Compound **18** (150 mg) was isolated from Fr. 4-3-4 by recrystallization. Meanwhile, compounds **20** (7.1 mg, *t_R* 24 min), **14** (4.3 mg, *t_R* 15 min) and **6** (141 mg, *t_R* 25 min) were isolated from Frs. 4-3-6, 4-3-7, 4-3-8 by semiprep-HPLC with 55% MeOH (2.5 mL/min), 50% MeCN (2.3 mL/min), and 68% MeCN (1.4 mL/min) elutions, respectively. Besides, compounds **27** (2 mg, *t_R* 10 min) and **26** (2.2 mg, *t_R* 12 min) was purified from Fr.4-4 and Fr. 4-6 by semiprep-HPLC with 80% MeOH (2.5 mL/min) and 60% MeCN (2.3 mL/min) elutions, respectively. Fraction 5 (4 g) was subjected to Sephadex LH-20 (MeOH) to provide five subfractions (Frs.5-1~5-5). Fr. 5-4 was further purified on semiprep-HPLC by 66% MeCN (2.5 mL/min) to give compounds **8** (77 mg, *t_R* 9 min), **12** (4 mg, *t_R* 11.5 min), and **7** (142 mg, *t_R* 20.6 min). Seven subfractions (Frs.7-1~7-7) were obtained from Fr. 7 (4 g) by Sephadex LH-20 (MeOH). Then Fr. 7-4 was subjected to an ODS column (MeOH/H₂O: 10–100%) to provide thirteen subfractions (Frs.7-4-1~7-4-13). Fr. 7-4-8 was further purified on semiprep-HPLC by 47% MeCN (2.5 mL/min) to give compounds **4** (2.3 mg, *t_R* 12 min), **10** (2 mg, *t_R* 16 min), and **2** (3.8 mg, *t_R* 39 min), along with one subfraction (Fr. 7-4-8-6). Compounds **11** (4.7 mg, *t_R* 42 min) and

1 (24 mg, *t_R* 45 min) were purified from Fr. 7-4-8-6 by semiprep-HPLC by 56% MeOH (2.3 mL/min). Fr. 7-4-12 was subjected to semiprep-HPLC (74%MeOH, 1.8 mL/min) to give compounds **16** (2.6 mg, *t_R* 14 min) and **15** (3.8 mg, *t_R* 45 min). Similarly, Fr. 7-5 was subjected to an ODS column (MeOH/H₂O: 10–100%) to provide eight subfractions (Frs.7-5-1~7-5-8). Compounds **19** (5.6 mg, *t_R* 10.4 min) and **28** (5 mg, *t_R* 8 min) were purified from Fr.7-5-5 and Fr.7-5-6 by semiprep-HPLC with 50% MeCN (2.5 mL/min) and 47% MeCN (2.5 mL/min) elutions, respectively. Fr. 7-5-7 was subjected to semiprep-HPLC (50%MeCN, 2.5 mL/min) to afford compounds **22** (5 mg, *t_R* 11.5 min) and **21** (1.5 mg, *t_R* 15 min). Fr.9 (7 g) was subjected to Sephadex LH-20 (MeOH) and followed by an ODS column (MeOH/H₂O: 10–100%) to provide six subfractions (Frs.9-1-1~9-1-6). Fr. 9-1-4 was purified by semiprep-HPLC (55%MeCN, 2.0 mL/min) to provide compounds **9** (3 mg, *t_R* 12 min), **5** (3 mg, *t_R* 25 min), **3** (2 mg, *t_R* 28 min). Compound **13** (0.8 mg, *t_R* 10 min) was isolated from Fr.9-1-5 by semiprep-HPLC (78% MeOH, 2.0 mL/min).

Antiviral Activity

All the isolated compounds (**1–28**), along with recently reported co-isolated 5-chloroisorotiorin (Luo et al., 2018), were screened for their anti-IAV activities according to the previously reported 3-(4,5-dimethylthiazol-2-yl)-2,5-diphenyltetrazolium bromide (MTT) colorimetric assay, using ribavirin as a positive control (Li et al., 2017; Yang et al., 2018). In brief, Madin Derby canine kidney (MDCK) cells were cultured in Dulbecco's modified Eagle's medium (DMEM) supplemented with 10% fetal bovine serum and 1% penicillin/streptomycin. Meanwhile, different

influenza A virus subtypes, including A/Puerto Rico/8/34 H274Y (H1N1), A/FM-1/1/47 (H1N1), and A/Aichi/2/68 (H3N2), were multiplied in 10-day-old chick embryo at 37°C. The cytotoxicity of the compounds was also evaluated by the MTT assay. Briefly, approximately 90% confluent cells in 96-well plates were exposed to the compounds at 2-fold serial dilutions. After 48 h of incubation, 100 μ L of MTT solution, which was diluted by the medium to 0.5 mg/mL, was added and retained at 37°C for 4 h. Then the supernatant was removed, followed by the addition of 150 μ L of dimethyl sulfoxide (DMSO) to dissolve the formazan product. The optical density for each well was measured on the Tecan Genios Pro microplate reader (Bedford, MA, USA) at 570 nm. To determine the antiviral activities of the compounds, confluent MDCK cells were infected with the virus at multiplicity of infection (MOI) of 0.01 at 37°C for 1 h. The compounds of non-cytotoxic concentrations were then added to the cells after washing away the unabsorbed virus with phosphate-buffered saline (PBS), and the cells were cultured for another 48 h. At the end of the culture, the MTT-based assay as previously described was assessed for the antiviral activity of the isolated compounds.

Statistical Analysis

All statistical analysis of the data were processed by GraphPad Prism. The results are presented as the mean \pm standard deviation (SD) from experiments in triplicate. Student's *t*-test was used to analyze the statistical significance between two groups, more groups by one-way ANOVA with or without Tukey–Kramer multiple comparison. A *p* < 0.05 was regarded as statistically significant.

RESULTS AND DISCUSSION

Identification of Compounds

The endophytic fungus *Diaporthe* sp. SCSIO 41011 was cultured on solid rice medium for 60 days. The EtOAc extract (150 g) of the fermentation was separated by continuously silica gel chromatography and semi-preparative HPLC chromatography to yield 28 aromatic polyketides (1–28). Their chemical structures

were determined by comprehensive spectroscopic analyses or comparison with those reported data.

Compound **1** was obtained as colorless oil and had the molecular formula C₁₉H₂₆O₇ as determined by a deprotonated ion peak at *m/z* 365.1607 (calcd for C₁₉H₂₅O₇, 365.1600) in HRESIMS data. The ¹H NMR data (Table 1) along with HSQC experiment of **1** displayed two singlet methyls at δ_{H} 2.01 (3H, s) and 3.65 (3H, s), two aromatic protons at δ_{H} 6.26 (1H, d, *J* = 2.2 Hz) and 6.19 (1H, d, *J* = 2.2 Hz), along with an array of methylene signals. The ¹³C NMR spectrum (Table 1) showed 19 resonances that were sorted by a distortionless enhancement by polarization transfer (DEPT) experiment, assigned to three carbonyls (δ_{C} 209.0, 174.0, and 173.1), six aromatic carbons (δ_{C} 161.8, 160.1, 137.0, 120.9, 112.0, and 102.9), eight methylenes (δ_{C} 65.7, 45.0, 40.4, 30.3, 30.1, 29.6, 26.8, and 25.4) and two methyls (δ_{C} 52.3 and 20.8). The aforementioned NMR data showed **1** was closely related structurally to the co-isolated 16-acetoxydothiorelone C (**3**) (Liu et al., 2018). The only difference was the appearance of a methyl group ($\delta_{\text{H/C}}$ 3.65/52.3) at C-1' in **1** instead of an ethyl group in **3**, which was also verified by the HMBC correlation from H₃-1' to C-1 (Figure 2). Thus, the structure of **1** was determined as shown in Figure 1 and assigned the trivial name dothiorelone O.

Compound **2** was also acquired as colorless oil and was determined to have the molecular formula C₂₀H₂₈O₇ from the HRESIMS data. Inspection of the comprehensive spectral data of **2**, including MS, and 1D, 2D-NMR data, indicated that **2** shared the same planer structure with (15*S*)-acetoxydothiorelone A (Liu et al., 2018). Comparison of the specific rotations between **2** ($[\alpha]_{\text{D}}^{25} = -5.8$ (c 0.10, MeOH)) and (15*S*)-acetoxydothiorelone A ($[\alpha]_{\text{D}}^{20} = +4.9$ (c 0.25, MeOH)) suggested **2** had the 15*R* configuration (Izuchi et al., 2011; Beekman and Barrow, 2015; Liu et al., 2018), given that they possessed only one chiral carbon at C-15. Therefore, the structure of **2** was resolved and accordingly named (15*R*)-acetoxydothiorelone A.

Compound **13** was also isolated as colorless oil and gave a molecular formula of C₁₈H₂₂O₅ relied on a deprotonated ion peak at *m/z* 317.1403 (calcd for C₁₈H₂₁O₅, 317.1389) in the HRESIMS spectrum. The ¹H NMR data (Table 1) together with

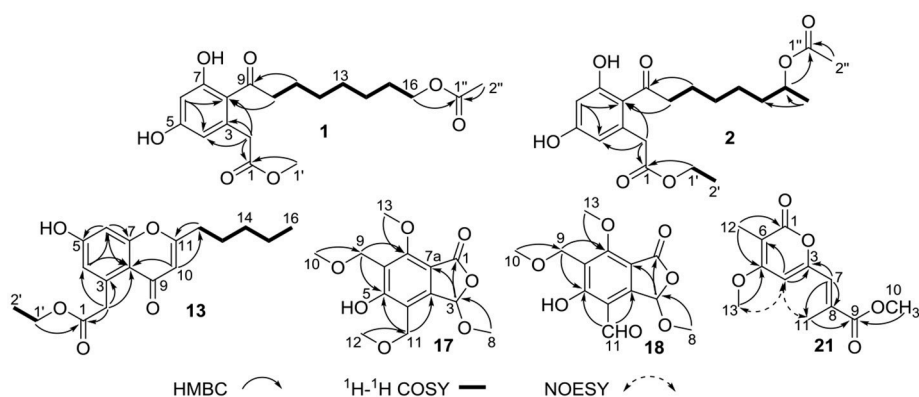


FIGURE 2 | Key HMBC, ¹H-¹H COSY, and NOESY correlations of compounds **1–2**, **13**, **17–18**, and **21**.

TABLE 1 | ^1H and ^{13}C NMR spectral data of compounds **1**, **2**, and **13** in CD_3OD .

| No. | 1 | | 2 | | 13 | |
|-----|-----------------------|---|-----------------------|---|-----------------------|---|
| | δ_{H}^a | δ_{C} , type ^b | δ_{H}^c | δ_{C} , type ^d | δ_{H}^c | δ_{C} , type ^d |
| 1 | | 174.0, C | | 173.6, C | | 173.6, C |
| 2 | 3.58, s | 40.4, CH ₂ | 3.60, s | 40.6, CH ₂ | 4.06, s | 42.1, CH ₂ |
| 3 | | 137.0, C | | 137.1, C | | 138.5, C |
| 4 | 6.19, d (2.2) | 112.0, CH | 6.21, d (2.2) | 111.9, CH | 6.65, d (2.2) | 120.3, CH |
| 5 | | 161.8, C | | 161.6, C | | 164.8, C |
| 6 | 6.26, d (2.2) | 102.9, CH | 6.28, d (2.2) | 102.8, CH | 6.73, d (2.2) | 103.1, CH |
| 7 | | 160.1, C | | 160.0, C | | 161.5, C |
| 8 | | 120.9, C | | 121.1, C | | 115.1, C |
| 9 | | 209.0, C | | 208.9, C | | 181.4, C |
| 10 | 2.85, t (7.6) | 45.0, CH ₂ | 2.83, t (7.6) | 43.3, CH ₂ | 5.98, s | 110.3, CH |
| 11 | 1.61, m | 25.4, CH ₂ | 1.62, o | 25.3, CH ₂ | | 170.3, C |
| 12 | 1.34, o | 30.3, CH ₂ | 1.35, o | 30.2, CH ₂ | 2.61, t (7.1) | 34.5, CH ₂ |
| 13 | 1.34, o | 30.1, CH ₂ | 1.35, o | 26.3, CH ₂ | 1.73, m | 27.6, CH ₂ |
| 14 | 1.34, o | 26.8, CH ₂ | 1.52, m | 36.8, CH ₂ | 1.39, o | 32.3, CH ₂ |
| 15 | 1.61, m | 29.6, CH ₂ | 4.86, o | 72.4, CH | 1.39, o | 23.4, CH ₂ |
| 16 | 4.04, t (7.1) | 65.7, CH ₂ | 1.22, d (7.1) | 20.2, CH ₃ | 0.93, t (7.1) | 14.2, CH ₃ |
| 1' | 3.65, s | 52.3, CH ₂ | 4.14, q (7.1) | 61.8, CH ₂ | 4.13, q (7.1) | 61.7, CH ₂ |
| 2' | | | 1.26, t (7.1) | 14.5, CH ₃ | 1.24, t (7.1) | 14.5, CH ₃ |
| 1'' | | 173.1, C | | 172.8, C | | |
| 2'' | 2.01, s | 20.8, CH ₃ | 2.02, s | 21.2, CH ₃ | | |

^aIn 500 MHz.^bIn 125 MHz.^cIn 700 MHz.^dIn 175 MHz, m, multiplet; o, overlapped.

HSQC and HMBC spectra of **13** displayed signals indicative of two doublet methyls at δ_{H} 0.93 (3H, d, $J = 7.1$ Hz) and 1.24 (3H, d, $J = 7.1$ Hz), three aromatic protons at δ_{H} 6.65 (1H, d, $J = 2.2$ Hz), 6.73 (1H, d, $J = 2.2$ Hz) and 5.98 (1H, s), along with several methylenes. The ^{13}C NMR spectrum (Table 1) showed 18 resonances attributable to two carbonyls (δ_{C} 173.6 and 181.4), six aromatic carbons (three oxygenated ones), six methylenes (δ_{C} 61.7, 42.1, 34.5, 32.3, 27.6, and 23.4) and two methyls (δ_{C} 14.2 and 14.5). The above mentioned spectral characteristics were closely consistent to those of the isolated pestalotiopson F (**14**) (Xu et al., 2009a), but suggested the appearance of an ethyl group ($\delta_{\text{H/C}}$ 4.13/61.7 at C-1' and 1.24/14.5 at C-2') in **13** rather than a methyl group ($\delta_{\text{H/C}}$ 3.66/52.2) at C-1' in **14**. These changes were also ascertained by the HMBC correlations from H₃-1' to C-1 and from H₃-2' to C-1', as well as the ^1H - ^1H COSY correlation of H₃-2' and H₂-1' (Figure 2). Based on the above discussion, the structure of **13** was elucidated and the trivial name pestalotiopson H was assigned.

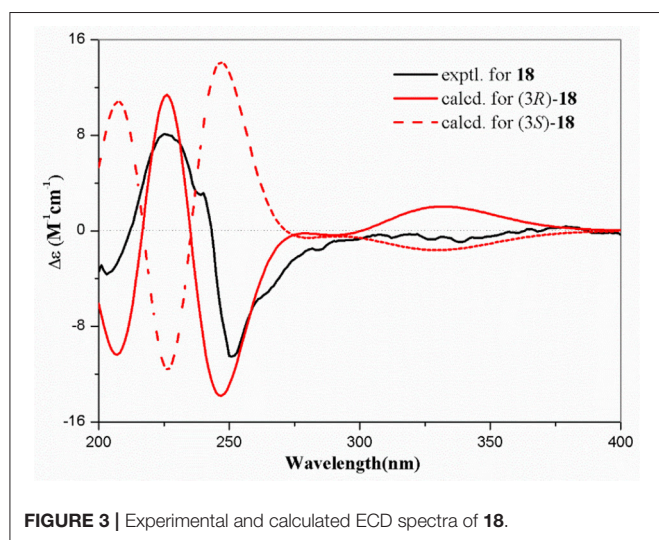
Compound **17** was obtained as a white solid and its molecular formula was found to be C₁₄H₁₈O₇ on the basis of HRESIMS and NMR data. The ^1H NMR data (Table 2) of **17** revealed four *O*-methyls at δ_{H} 3.38, 3.38, 3.54, and 3.99, two singlet methylenes at δ_{H} 4.60 and 4.65, and a hemiketal methine at δ_{H} 6.29. In addition to the above seven corresponding hydrogen-bearing carbons, seven carbons remained in the ^{13}C NMR spectrum,

including one carbonyl (δ_{C} 169.6), six aromatic carbons [(δ_{C} 111.4, 119.0, 121.4, 148.9), and two oxygenated ones at δ_{C} 160.7 and 174.3]. The foregoing spectroscopic data showed great similarity to that of microsphaerophthalide F (Sommar et al., 2012) except that a methyl group ($\delta_{\text{H/C}}$ 2.16/8.5) located at C-6 in microsphaerophthalide F was replaced by an ethoxyl group ($\delta_{\text{H/C}}$ 4.60/65.3 at C-9 and 3.38/58.1 at C-10) anchored at C-6 in **17**. This deduction was also supported by the HMBC correlations from H₃-10 to C-9 and from H₂-9 to C-5 and C-7. The barely measurable optical rotation value and quite weak Cotton effects in the ECD spectrum suggested **17** was racemic, which was also confirmed by the chiral HPLC analysis with two peaks (peak area ratio: 1:1) in the HPLC profile (Supplementary Materials). However, the quantity of **17** was too little to perform further resolution. Hence, the structure of compound **17** was elucidated and the trivial name (\pm)-microsphaerophthalide H was assigned.

Compound **18** was obtained as colorless needle crystals and had the molecular formula C₁₃H₁₄O₇, as evidenced by HRESIMS ([M+H]⁺, 283.0809; calcd for C₁₃H₁₅O₇, 283.0818) and the NMR data. The highly similar NMR spectroscopic data of **18** to those of **17** indicated that their structures were closely related, except for the presence of an aldehyde group ($\delta_{\text{H/C}}$ 10.14/192.5) joined at C-4 in **18**, rather than an ethoxyl group ($\delta_{\text{H/C}}$ 4.65/67.2 and 3.38/58.4) anchored at C-4 in **17**. The absolute configuration of C-3 of **18** was mainly determined by comparison of the specific rotations with those reported data, as well as comparison between

TABLE 2 | ^1H and ^{13}C NMR spectral data of compounds **17**, **18** and **21** (^1H for 700 MHz, ^{13}C for 175 MHz).

| No. | 17 ^a | | 18 ^b | | 21 ^a | |
|-----|---------------------|----------------------------|---------------------|----------------------------|---------------------|----------------------------|
| | δ_{H} | δ_{C} , type | δ_{H} | δ_{C} , type | δ_{H} | δ_{C} , type |
| 1 | | 169.6, C | | 164.7, C | | 166.3, C |
| 2 | | | | | | |
| 3 | 6.29, s | 103.1, CH | 6.75, s | 100.7, CH | | 158.8, C |
| 3a | | 148.9, C | | 151.7, C | | |
| 4 | | 119.0, C | | 112.4, C | 6.87, d (1.4) | 98.8, CH |
| 5 | | 174.3, C | | 166.3, C | | 167.8, C |
| 6 | | 121.4, C | | 120.9, C | | 105.6, C |
| 7 | | 160.7, C | | 163.1, C | 6.67, s | 120.3, CH |
| 7a | | 111.4, C | | 109.6, C | | |
| 8 | 3.54, s | 56.1, CH ₃ | 3.60, s | 56.9, CH ₃ | | 144.5, C |
| 9 | 4.60, s | 65.3, CH ₂ | 4.44, s | 61.3, CH ₂ | | 168.0, C |
| 10 | 3.38, s | 58.1, CH ₃ | 3.27, s | 57.7, CH ₃ | 3.76, s | 52.0, CH ₃ |
| 11 | 4.65, s | 67.2, CH ₂ | 10.14, s | 192.5, CH | 2.44, d (1.4) | 13.6, CH ₃ |
| 12 | 3.38, s | 58.4, CH ₃ | | | 1.92, s | 8.8, CH ₃ |
| 13 | 3.99, s | 63.0, CH ₃ | 4.14, s | 63.4, CH ₃ | 4.02, s | 57.5, CH ₃ |

^aIn CD₃OD.^bIn DMSO-d₆.**FIGURE 3** | Experimental and calculated ECD spectra of **18**.

the computed and experimental ECD spectra. Among these reported 3-oxygenated phthalides, the 3*S*- and 3*R*- ones generally showed negative and positive specific rotations, respectively (Sommat et al., 2012). Thus, the positive sign of specific rotation $[[\alpha]_D^{25} = +25$ (c 0.10, MeOH)] of **18** led to the deduction of 3*R* configuration in **18**, which was also confirmed from experimental and calculated ECD spectra of **18** as shown in **Figure 3**. Further chiral HPLC analysis confirmed that **18** was single enantiomer. Consequently, the structure of **18** was determined as shown in **Figure 1** and termed microsphaerophthalide I. Notably, the 3-oxygenated phthalides are uncommon in natural sources.

Compound **21** was obtained as a white solid and had the molecular formula C₁₂H₁₄O₅, as determined from HRESIMS

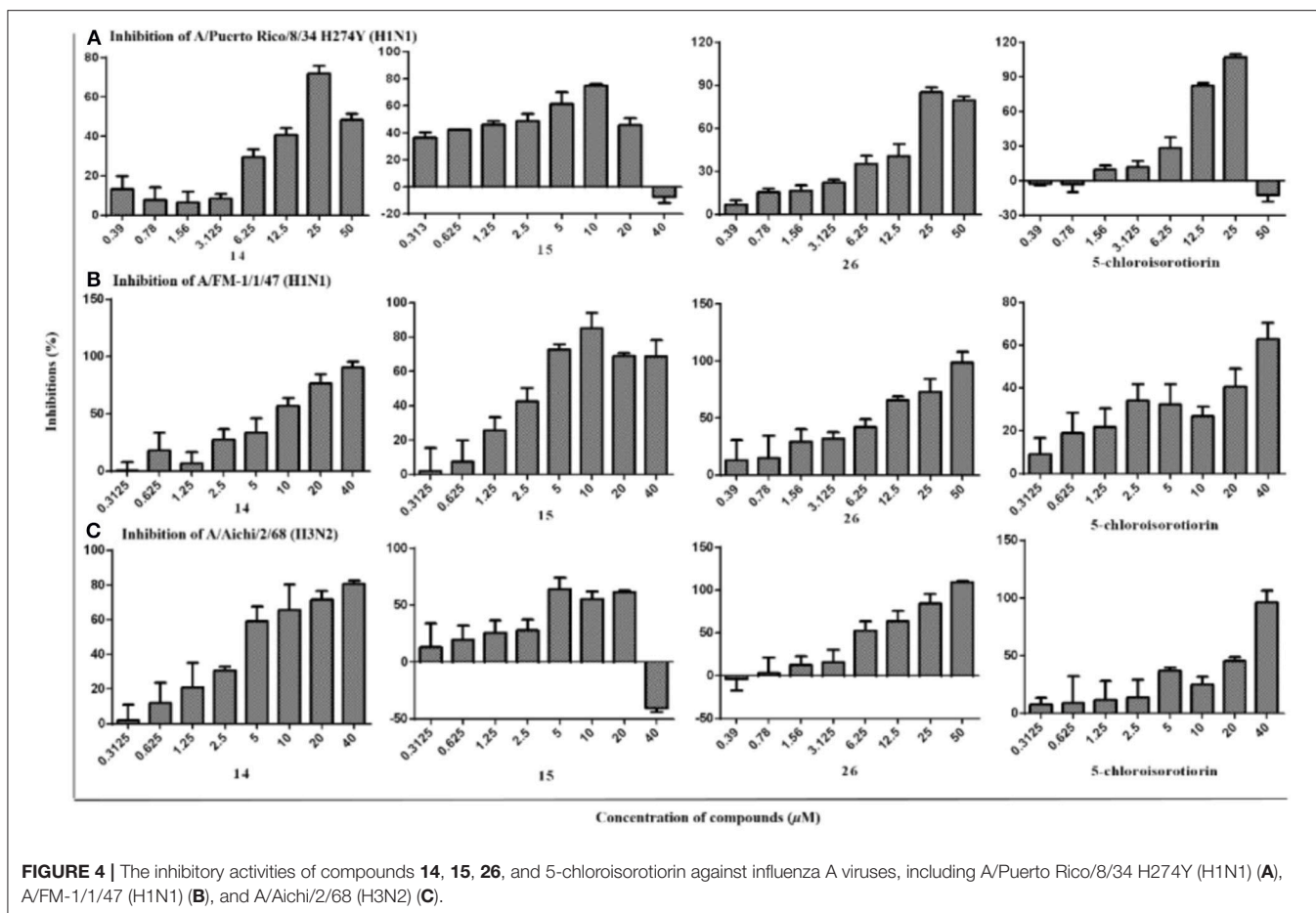
TABLE 3 | Inhibition activity of compounds **1–28** and 5-chloroisorotiorin against Influenza A Virus strains.

| Compounds | IC ₅₀ (μM) ^a | | |
|---------------------|------------------------------------|--------------------|---------------------|
| | A/Puerto Rico/8/34 H274Y (H1N1) | A/FM-1/1/47 (H1N1) | A/Aichi/2/68 (H3N2) |
| 14 | 21.80 ± 7.96 | 6.74 ± 1.26 | 6.17 ± 1.46 |
| 15 | 2.56 ± 0.32 | 4.82 ± 1.90 | 6.76 ± 2.72 |
| 26 | 9.40 ± 1.96 | 4.80 ± 1.28 | 5.12 ± 1.49 |
| 5-chloroisorotiorin | 2.52 ± 0.21 | 37.97 ± 15.11 | 10.10 ± 1.84 |
| Remainings | IN ^b | IN | IN |

^aThe samples were tested in triplicate, and the data are presented as the mean ± SD^bInactive.

($[\text{M}+\text{H}]^+$, 239.0917; calcd for C₁₂H₁₅O₅, 239.0919) and the NMR data. Detailed analyses of its NMR spectroscopic features implied that it was closely related structurally to convolvulopyrone (Tsantrizos et al., 1992), but for the presence of an additional *O*-methyl group ($\delta_{\text{H}/\text{C}}$ 3.76/52.0) at C-10 in **21**, indicating that **21** was a methyl derivative of convolvulopyrone. Besides, compound **21** and convolvulopyrone shared the same relative configuration of 7*E* due to the absence of a NOESY correlation between H-7 and H₃-11. As a result, the structure of **21** was determined and given the trivial name methyl convolvulopyrone. However, compound **21** was likely obtained as an artifact formed in the process of extraction and purification using MeOH as a solvent.

Besides, these co-isolated known congeners were elucidated by comparing their physicochemical properties and spectroscopic data with those reported literature values (Supplementary Materials). They were determined as 16-acetoxydothiarelone C (**3**) (Liu et al., 2018), dothiarelone C (**4**) (Liu et al., 2018),



(14*R*)-acetoxydothiarelone B (**5**) (Liu et al., 2018), cytosporone N (**6**) (Beekman and Barrow, 2015), cytosporone B (**7**) (Brady et al., 2000), cytosporone A (**8**) (Brady et al., 2000), dothiarelone I (**9**) (Liu et al., 2018), (15*R*)-dothiarelone A (**10**) (Liu et al., 2018), methyl (*R*)-2-(2-(7-acetoxyoctanoyl)-3,5-dihydroxyphenyl)acetate (**11**) (Beekman and Barrow, 2015), secocurvarulin (**12**) (Bracher and Krauss, 1998), pestalotiopsone F (**14**) (Xu et al., 2009a), pestalotiopsone B (**15**) (Xu et al., 2009a), pestalotiopsone A (**16**) (Xu et al., 2009a), 5-hydroxy-7-methoxy-4,6-dimethylphthalide (**19**) (Sommar et al., 2012), dihydrovermistatin (**20**) (Komai et al., 2005), sclerotinin A (**22**) (Lai et al., 2013), 3,5-dimethyl-8-hydroxy-3,4-dihydroisocoumarin (**23**) (Kokubun et al., 2003), 3,5-dimethyl-8-methoxy-3,4-dihydroisocoumarin (**24**) (Kokubun et al., 2003), methyl 8-hydroxy-6-methyl-9-oxo-9*H*-xanthene-1-carboxylate (**25**) (Lai et al., 2013), 3,8-dihydroxy-6-methyl-9-oxo-9*H*-xanthene-1-carboxylate (**26**) (Nguyen et al., 2017), pinselin (**27**) (Cui et al., 2016), 7-hydroxy-2,5-dimethylchromone (**28**) (Koenigs et al., 2010). Amongst, methyl (*R*)-2-[2-(7-acetoxyoctanoyl)-3,5-dihydroxyphenyl]acetate (**11**) was isolated as a naturally occurring compound for the first time. While sclerotinin A (**22**) was isolated as a diastereoisomeric mixture which could not be separated by RP-HPLC method (Lai et al., 2013). This research further enriched secondary

metabolites in the genus *Diaporthe* and also expanded the chemical diversity of polyketides, such as dothiarelones, cytosporones, phthalides, chromones, etc.

Antiviral Activity

Antiviral effect of the isolated compounds **1–28** and 5-chloroisorotiorin against different IAV subtypes, including A/Puerto Rico/8/34 H274Y (H1N1), A/FM-1/1/47 (H1N1), and A/Aichi/2/68 (H3N2), were then evaluated. Those compounds showed nearly no cytotoxicity against MDCK cells ($IC_{50} > 200 \mu M$). Compounds **14**, **15**, **26**, and 5-chloroisorotiorin displayed significant anti-IAV activities against the above mentioned subtypes with IC_{50} values in the range of 2.52–39.97 μM (Table 3). However, the remaining compounds (**1–13**, **16–25**, **27–28**) were inactive toward the three aforementioned IAV subtypes. Furthermore, pestalotiopsone F (**14**) and 3,8-dihydroxy-6-methyl-9-oxo-9*H*-xanthene-1-carboxylate (**26**) exhibited obvious inhibition effect on A/FM-1/1/47 (H1N1), as well as A/Aichi/2/68 (H3N2), in a dose-dependent manner (Figure 4).

Additionally, based on comparison of the structural characteristics among these analogs, a preliminary structure-activity relationship is discussed. Pestalotiopsone F (**14**) exhibited selective inhibitions against the two IAV subtypes

of A/FM-1/1/47 (H1N1) and A/Aichi/2/68 (H3N2) with the IC_{50} values of 6.74 ± 1.26 and $6.17 \pm 1.46 \mu\text{M}$, respectively. Comparing with the antiviral pestalotiopsone F (**14**) and B (**15**), the co-isolated siblings pestalotiopsone H (**13**) and A (**16**) were inactive toward the three IAV subtypes, which revealed methylation of the carboxyl group at C-1 for the pestalotiopsone with a C_7 aliphatic branch located at C-11, and while ethylation of the carboxyl group at C-1 for the pestalotiopsone with a C_5 aliphatic branch located at C-11, were essential for anti-IAV activities. Notably, among the three xanthenes (**25–27**), only 3,8-dihydroxy-6-methyl-9-oxo-9*H*-xanthene-1-carboxylate (**26**) demonstrated remarkable inhibitory effects against A/FM-1/1/47 (H1N1), A/Puerto Rico/8/34 H274Y (H1N1), and A/Aichi/2/68 (H3N2) with IC_{50} values of 4.80 ± 1.28 , 9.40 ± 1.96 , and $5.12 \pm 1.49 \mu\text{M}$, respectively, which indicated the hydroxyl group at C-3 probably promote the anti-IAV activities toward the three subtypes. By the way, 5-chloroisorotiorin (Luo et al., 2018), a recently reported co-isolated chloroazaphilone derivative obtained with major amount, was also screened for anti-IAV activity, which presented selective inhibition activities against the two IAV subtypes of A/Puerto Rico/8/34 H274Y (H1N1) and A/Aichi/2/68 (H3N2) with the IC_{50} values of 2.52 ± 0.21 and $10.10 \pm 1.84 \mu\text{M}$, respectively. The remaining ones (**1–13**, **16–26**, **27–28**) showed no obvious inhibition against A/FM-1/1/47 (H1N1), A/Puerto Rico/8/34 H274Y (H1N1), and A/Aichi/2/68 (H3N2).

Characterization of Compounds

Dothiorelone O (**1**): colorless oil; UV (MeOH) λ_{max} (log ϵ) 302 (3.75), 269 (3.89), 220 (4.16), 204 (4.27) nm; IR (film) ν_{max} 3,356, 2,933, 2,833, 1,732, 1,714, 1,609, 1,591, 1,462, 1,261, 1,163, and 1,028 cm^{-1} ; ^1H and ^{13}C NMR data, **Table 1**; HRESIMS m/z 365.1607 $[\text{M}-\text{H}]^-$ (calcd for $\text{C}_{19}\text{H}_{25}\text{O}_7$, 365.1600), 401.1368 $[\text{M}+\text{Cl}]^-$ (calcd for $\text{C}_{19}\text{H}_{26}\text{ClO}_7$, 401.1367).

(15*R*)-acetoxidothiorelone A (**2**): colorless oil; $[\alpha]_D^{25} - 5.8$ (c 0.10, MeOH); UV (MeOH) λ_{max} (log ϵ) 303 (3.69), 269 (3.78), 220 (4.14), 204 (4.17) nm; IR (film) ν_{max} 3,358, 2,933, 2,858, 1,732, 1,714, 1,609, 1,558, 1,456, 1,265, 1,249, 1,159, and 1,024 cm^{-1} ; ^1H and ^{13}C NMR data, **Table 1**; HRESIMS m/z 403.1741 $[\text{M}+\text{Na}]^+$ (calcd for $\text{C}_{20}\text{H}_{28}\text{NaO}_7$, 403.1733), 419.1470 $[\text{M}+\text{K}]^+$ (calcd for $\text{C}_{20}\text{H}_{28}\text{KO}_7$, 419.1472), 783.3563 $[\text{2M}+\text{Na}]^+$ (calcd for $\text{C}_{40}\text{H}_{56}\text{NaO}_{14}$, 783.3568).

Pestalotiopsone H (**13**): colorless oil; UV (MeOH) λ_{max} (log ϵ) 291 (4.14), 250 (4.31), 242 (4.28), 217 (4.38) nm; IR (film) ν_{max} 3,419, 2,927, 2,856, 1,732, 1,716, 1,645, 1,558, 1,456, 1,375, 1,274, 1,180, 1,161, and 1,028 cm^{-1} ; ^1H and ^{13}C NMR data, **Table 1**; HRESIMS m/z 317.1403 $[\text{M}-\text{H}]^-$ (calcd for $\text{C}_{18}\text{H}_{21}\text{O}_5$, 317.1389), 353.1167 $[\text{M}+\text{Cl}]^-$ (calcd for $\text{C}_{18}\text{H}_{22}\text{ClO}_5$, 353.1156), 635.2860 $[\text{2M}-\text{H}]^-$ (calcd for $\text{C}_{36}\text{H}_{43}\text{O}_{10}$, 635.2856), 671.2626 $[\text{2M}+\text{Cl}]^-$ (calcd for $\text{C}_{36}\text{H}_{44}\text{ClO}_{10}$, 671.2623).

(\pm)-microsphaerophthalide H (**17**): a white solid; $[\alpha]_D^{25} - 5$ (c 0.06, MeOH); UV (MeOH) λ_{max} (log ϵ) 307 (4.06), 249 (4.05), 220 (4.48) nm; IR (film) ν_{max} 3,419, 2,935, 2,846, 1,747, 1,734, 1,604, 1,558, 1,448, 1,429, 1,375, 1,276, 1,201, 1,159, 1,093, and 1,074 cm^{-1} ; ^1H and ^{13}C NMR data, **Table 2**; HRESIMS m/z 299.1123 $[\text{M}+\text{H}]^+$ (calcd for $\text{C}_{14}\text{H}_{19}\text{O}_7$, 299.1131),

321.0954 $[\text{M}+\text{Na}]^+$ (calcd for $\text{C}_{14}\text{H}_{18}\text{NaO}_7$, 321.0950), 619.2010 $[\text{2M}+\text{Na}]^+$ (calcd for $\text{C}_{28}\text{H}_{36}\text{NaO}_{14}$, 619.2003).

Microsphaerophthalide I (**18**): colorless needle crystals; $[\alpha]_D^{25} = +25$ (c 0.10, MeOH); UV (MeOH) λ_{max} (log ϵ) 367 (3.60), 295 (4.07), 245 (4.46), 201 (4.10) nm; ECD (0.15 mg/mL, MeOH) λ_{max} ($\Delta\epsilon$) 203 (−2.07), 225 (+4.62), 251 (−6.00) nm; IR (film) ν_{max} 3,419, 2,945, 2,885, 1,770, 1,749, 1,668, 1,653, 1,558, 1,489, 1,375, 1,338, 1,286, 1,205, 1,097, and 1,058 cm^{-1} ; ^1H and ^{13}C NMR data, **Table 2**; HRESIMS m/z 283.0809 $[\text{M}+\text{H}]^+$ (calcd for $\text{C}_{13}\text{H}_{15}\text{O}_7$, 283.0818), 305.0632 $[\text{M}+\text{Na}]^+$ (calcd for $\text{C}_{13}\text{H}_{14}\text{NaO}_7$, 305.0637).

Methyl convulvolopyrone (**21**): a white solid; UV (MeOH) λ_{max} (log ϵ) 343 (4.05), 279 (3.73), 239 (4.51), 205 (4.12) nm; IR (film) ν_{max} 3,446, 2,954, 2,927, 1,681, 1,635, 1,446, 1,355, 1,195, 1,182, 1,139, and 1,039 cm^{-1} ; ^1H and ^{13}C NMR data, **Table 2**; HRESIMS m/z 239.0917 $[\text{M}+\text{H}]^+$ (calcd for $\text{C}_{12}\text{H}_{15}\text{O}_5$, 239.0919), 261.0749 $[\text{M}+\text{Na}]^+$ (calcd for $\text{C}_{12}\text{H}_{14}\text{NaO}_5$, 261.0739), 499.1590 $[\text{2M}+\text{Na}]^+$ (calcd for $\text{C}_{24}\text{H}_{28}\text{NaO}_{10}$, 499.1580).

CONCLUSIONS

Twenty-eight aromatic polyketides, including two new octaketides (**1–2**), one new chromone derivative (**13**), two new highly substituted phthalides (**17–18**), and one new α -pyrone derivative (**21**) along with 22 known congeners were isolated from a mangrove-associated fungus *Diaporthe* sp. SCSIO 41011, while methyl (*R*)-2-[2-(7-acetoxyoctanoyl)-3,5-dihydroxyphenyl]acetate (**11**) was isolated as a new natural compound and (\pm)-microsphaerophthalide H (**17**) was obtained as a racemic mixture. Amongst, pestalotiopsone F (**14**), pestalotiopsone B (**15**), 3,8-dihydroxy-6-methyl-9-oxo-9*H*-xanthene-1-carboxylate (**26**), and 5-chloroisorotiorin displayed pronounced anti-IAV activities against three IAV virus subtypes, including A/Puerto Rico/8/34 H274Y (H1N1), A/FM-1/1/47 (H1N1), and A/Aichi/2/68 (H3N2) with IC_{50} values in the range of 2.52–39.97 μM . This work further enriched the chemical and bioactive diversity of polyketides, such as dothiorelones, cytosporones, phthalides, chromones, etc. Furthermore, our findings provide a basis for further development and utilization of pestalotiopsone, xanthone, and chloroazaphilone derivatives as source of potential anti-IAV chemotherapy agents.

AUTHOR CONTRIBUTIONS

XiaL: designed the experiments and performed the isolation and characterization of all the compounds and wrote the manuscript; JY and FC: performed the antiviral experiment; XiuL: performed the isolation and purification of the fungal strain; CC: contributed to isolation of the compounds; XZ: designed the research work and wrote the manuscript; SL and YL: contributed in project design and manuscript preparation. All authors reviewed the manuscript and approved for submission.

ACKNOWLEDGMENTS

This work was supported by grants from the National Natural Science Foundation of China (81741154, 41476135, 21772210), National Major Scientific and Technological Special Project for Significant New Drugs Development (2018ZX09735001-002-003), the Natural Science Foundation of Guangdong Province (2014A030313765, 2016A030313591), Science and Technology Project of Guangdong Province (2016A020222009), and the Open Project of State Key

Laboratory of Organ Failure Research. We thank to Z. Xiao, C. Li and A. Sun, analytical facility center of South China Sea Institute of Oceanology, for recording NMR, and MS data.

SUPPLEMENTARY MATERIAL

The Supplementary Material for this article can be found online at: <https://www.frontiersin.org/articles/10.3389/fchem.2018.00282/full#supplementary-material>

REFERENCES

- Abreu, L. M., Phipps, R. K., Pfenning, L. H., Gotfredsen, C. H., Takahashi, J. A., and Larsen, T. O. (2010). Cytosporones O, P and Q from an endophytic *Cytospora* sp. *Tetrahedron Lett.* 51, 1803–1805. doi: 10.1016/j.tetlet.2010.01.110
- Bautista, E., Chorpitayusunondh, T., Gao, Z., Harper, S. A., Shaw, M., Uyeki, T. M., et al. (2010). Medical progress: clinical aspects of pandemic 2009 influenza A (H1N1) virus infection. *New Engl. J. Med.* 362, 1708–1719. doi: 10.1056/NEJMra1000449
- Beekman, A. M., and Barrow, R. A. (2015). Syntheses of cytosporones A, C, J, K, and N, metabolites from medicinal fungi. *Aust. J. Chem.* 68, 1583–1592. doi: 10.1071/CH15144
- Bracher, F., and Krauss, J. (1998). Total synthesis of secocurvularin, curvulin, and the corresponding carboxylic acids. A convenient application of the enzymatic hydrolysis of acid and base sensitive esters. *Nat. Prod. Lett.* 12, 31–34. doi: 10.1080/10575639808048867
- Brady, S. F., Wagenaar, M. M., Singh, M. P., Janso, J. E., and Clardy, J. (2000). The cytosporones, new octaketide antibiotics isolated from an endophytic fungus. *Org. Lett.* 2, 4043–4046. doi: 10.1021/ol006680s
- Crawford, J. M., and Townsend, C. A. (2010). New insights into the formation of fungal aromatic polyketides. *Nat. Rev. Microbiol.* 8, 879–889. doi: 10.1038/nrmicro2465
- Cui, X., Zhu, G., Liu, H., Jiang, G., Wang, Y., and Zhu, W. (2016). Diversity and function of the Antarctic krill microorganisms from *Euphausia superba*. *Sci. Rep.* 6:36496. doi: 10.1038/srep36496
- Egarnes, B., Blanchet, M. R., and Gosselin, J. (2017). Treatment with the NR4A1 agonist cytosporone B controls influenza virus infection and improves pulmonary function in infected mice. *PLoS ONE* 12:e0186639. doi: 10.1371/journal.pone.0186639
- Fujii, I. (2010). Functional analysis of fungal polyketide biosynthesis genes. *J. Antibiot.* 63, 207–218. doi: 10.1038/ja.2010.17
- Hang, L., Liu, N., and Tang, Y. (2016). Coordinated and iterative enzyme catalysis in fungal polyketide biosynthesis. *ACS Catal.* 6, 5935–5945. doi: 10.1021/acscatal.6b01559
- Izuchi, Y., Koshino, H., Hongo, Y., Kanomata, N., and Takahashi, S. (2011). Synthesis and structural revision of phomopsin B, a novel polyketide carrying a 10-membered cyclic-ether ring. *Org. Lett.* 13, 3360–3363. doi: 10.1021/ol2011117
- Koenigs, P., Rinker, B., Maus, L., Nieger, M., Rheinheimer, J., and Waldvogel, S. R. (2010). Structural revision and synthesis of altechromone A. *J. Nat. Prod.* 73, 2064–2066. doi: 10.1021/np1005604
- Kokubun, T., Veitch, N. C., Bridge, P. D., and Simmonds, M. S. J. (2003). Dihydroisocoumarins and a tetralone from *Cytospora eucalypticola*. *Phytochemistry* 62, 779–782. doi: 10.1016/S0031-9422(02)00606-4
- Komai, S., Hosoe, T., Itabashi, T., Nozawa, K., Yaguchi, T., Fukushima, K., et al. (2005). New vermistatin derivatives isolated from *Penicillium simplicissimum*. *Heterocycles* 65, 2771–2776. doi: 10.3987/COM-05-10523
- Kongprapan, T., Xu, X., Rukachaisirikul, V., Phongpaichit, S., Sakayaroj, J., Chen, J., et al. (2017). Cytosporone derivatives from the endophytic fungus *Phomopsis* sp PSU-H188. *Phytochem. Lett.* 22, 219–223. doi: 10.1016/j.phytol.2017.10.002
- Kornsakulkarn, J., Somyong, W., Supothina, S., Boonyuen, N., and Thongpanchang, C. (2015). Bioactive oxygen-bridged cyclooctadienes from endophytic fungus *Phomopsis* sp BCC 45011. *Tetrahedron* 71, 9112–9116. doi: 10.1016/j.tet.2015.10.015
- Lai, D., Broetz-Oesterhelt, H., Mueller, W. E., Wray, V., and Proksch, P. (2013). Bioactive polyketides and alkaloids from *Penicillium citrinum*, a fungal endophyte isolated from *Ocimum tenuiflorum*. *Fitoterapia* 91, 100–106. doi: 10.1016/j.fitote.2013.08.017
- Li, R., Liu, T., Liu, M., Chen, F., Liu, S., and Yang, J. (2017). Anti-influenza A virus activity of dendrobine and its mechanism of action. *J. Agr Food Chem.* 65, 3665–3674. doi: 10.1021/acs.jafc.7b00276
- Liu, M., Chen, F., Liu, T., Chen, F., Liu, S., and Yang, J. (2017). The role of oxidative stress in influenza virus infection. *Microbes Infect.* 19, 580–586. doi: 10.1016/j.micinf.2017.08.008
- Liu, Z., Zhao, J., Liang, X., Lv, X., Li, Y., Qu, J., et al. (2018). Dothiorelone derivatives from an endophyte *Diaporthe pseudomangiferaea* inhibit the activation of human lung fibroblasts MRC-5 cells. *Fitoterapia* 127, 7–14. doi: 10.1016/j.fitote.2018.04.009
- Luo, X., Lin, X., Tao, H., Wang, J., Li, J., Yang, B., et al. (2018). Isochromophilones A–F, cytotoxic chloroazaphilones from the marine mangrove endophytic fungus *Diaporthe* sp. SCSIO 41011. *J. Nat. Prod.* 81, 934–941. doi: 10.1021/acs.jnatprod.7b01053
- Luo, X., Zhou, X., Lin, X., Qin, X., Zhang, T., Wang, J., et al. (2017). Antituberculosis compounds from a deep-sea-derived fungus *Aspergillus* sp. SCSIO Ind09F01. *Nat. Prod. Res.* 31, 1958–1962. doi: 10.1080/14786419.2016.1266353
- Medina, R. A., and Garcia-Sastre, A. (2011). Influenza A viruses: new research developments. *Nat. Rev. Microbiol.* 9, 590–603. doi: 10.1038/nrmicro2613
- Moghadamtousi, S., Nikzad, S., Kadir, H., Abubakar, S., and Zandi, K. (2015). Potential antiviral agents from marine fungi: an overview. *Mar. Drugs* 13, 4520–4538. doi: 10.3390/md13074520
- Nguyen, T. T. N., Tran, H. Q., Kim, K. W., Kim, H. J., Sohn, J. H., Kang, D. G., et al. (2017). Anti-inflammatory effects of secondary metabolites isolated from the marine-derived fungal strain *Penicillium* sp SF-5629. *Arch. Pharm. Res.* 40, 328–337. doi: 10.1007/s12272-017-0890-5
- Sommart, U., Rukachaisirikul, V., Tadpetch, K., Sukpondma, Y., Phongpaichit, S., Hutadilok-Towatana, N., et al. (2012). Modiolin and phthalide derivatives from the endophytic fungus *Microsphaeropsis arundinis* PSU-G18. *Tetrahedron* 68, 10005–10010. doi: 10.1016/j.tet.2012.09.043
- Song, G., Shen, X., Li, S., Li, Y., Liu, Y., Zheng, Y., et al. (2015). Structure-activity relationships of 3-O-beta-chacotriosyl ursolic acid derivatives as novel H5N1 entry inhibitors. *Eur. J. Med. Chem.* 93, 431–442. doi: 10.1016/j.ejmech.2015.02.029
- Tan, Q. W., Fang, P. H., Ni, J. C., Gao, F., and Chen, Q. J. (2017). Metabolites produced by an endophytic *Phomopsis* sp and their anti-TMV activity. *Molecules* 22:E2073. doi: 10.3390/molecules22122073
- Tan, Y., Yang, B., Lin, X., Luo, X., Pang, X., Tang, L., et al. (2018). Nitrobenzoyl sesquiterpenoids with cytotoxic activities from a marine-derived *Aspergillus ochraceus* Fungus. *J. Nat. Prod.* 81, 92–97. doi: 10.1021/acs.jnatprod.7b00698
- Tsantrizos, Y. S., Ogilvie, K. K., and Watson, A. K. (1992). Phytotoxic metabolites of *Pomopsis onvolvulus*, a host-specific pathogen of *Feld bindweed*. *Can. J. Chem.* 70, 2276–2284. doi: 10.1139/v92-286
- Von Delius, M., Le, C. M., Ellinger, B., Kuzikov, M., Gul, S., and Dong, V. M. (2017). Synthesis and biological activity of octaketides from the cytosporone family. *Isr. J. Chem.* 57, 975–981. doi: 10.1002/ijch.201700023

- Xia, Z., Cao, X., Rico-Bautista, E., Yu, J., Chen, L., Chen, J., et al. (2013). Relative impact of 3- and 5-hydroxyl groups of cytosporone B on cancer cell viability. *Medchemcomm* 4, 332–339. doi: 10.1039/C2MD20243C
- Xu, J., Kjer, J., Sendker, J., Wray, V., Guan, H., Edrada, R., et al. (2009a). Chromones from the endophytic fungus *Pestalotiopsis* sp. isolated from the Chinese mangrove plant *Rhizophora mucronata*. *J. Nat. Prod.* 72, 662–665. doi: 10.1021/np800748u
- Xu, J., Kjer, J., Sendker, J., Wray, V., Guan, H., Edrada, R., et al. (2009b). Cytosporones, coumarins, and an alkaloid from the endophytic fungus *Pestalotiopsis* sp. isolated from the Chinese mangrove plant *Rhizophora mucronata*. *Bioorgan. Med. Chem.* 17, 7362–7367. doi: 10.1016/j.bmc.2009.08.031
- Yang, L. P., Gu, X. L., Chen, J. X., Yang, J., Tan, S. Y., and Duan, W. J. (2018). Chemical constituents from *Canarium album* Raeusch and their anti-influenza A virus activities. *J. Nat. Med.* 72, 808–815 doi: 10.1007/s11418-018-1208-8
- Zhan, Y., Du, X., Chen, H., Liu, J., Zhao, B., Huang, D., et al. (2008). Cytosporone B is an agonist for nuclear orphan receptor Nur77. *Nat. Chem. Biol.* 4, 548–556. doi: 10.1038/nchembio.106
- Zheng, K., Xie, C., and Hong, R. (2015). Bioinspired iterative synthesis of polyketides. *Front. Chem.* 3:32. doi: 10.3389/fchem.2015.00032

Conflict of Interest Statement: The authors declare that the research was conducted in the absence of any commercial or financial relationships that could be construed as a potential conflict of interest.

Copyright © 2018 Luo, Yang, Chen, Lin, Chen, Zhou, Liu and Liu. This is an open-access article distributed under the terms of the Creative Commons Attribution License (CC BY). The use, distribution or reproduction in other forums is permitted, provided the original author(s) and the copyright owner(s) are credited and that the original publication in this journal is cited, in accordance with accepted academic practice. No use, distribution or reproduction is permitted which does not comply with these terms.